

# Highly Selective Optical Detection in a Lab-on-a-Chip for Biological Fluids Analysis

Graça Minas, Júlio S. Martins and José H. Correia

University of Minho, Department of Industrial Electronics  
Campus de Azurém, 4800-058 Guimarães, Portugal

(Received March 29, 2001; accepted October 15, 2001)

**Key words:** lab-on-a-chip, microfluidics, proteins, Fabry-Perot filter, highly selective filter

This paper presents a microfluidic system for determining the protein concentrations in human biological fluids (*e.g.*, urine) with a highly sensitive and selective optical photodetector based on a Fabry-Perot filter. The microsystem consists of two wafers: a Pyrex glass wafer containing the microlaboratory (microchannels to carry chemical reagents and sample solutions) and a silicon wafer that includes the protein detection system and readout electronics. The optical channel operates in the visible spectral range. Optical simulations of the Fabry-Perot filter for narrow band operation are demonstrated by the determination of total protein and albumin concentration in urine. Compensation techniques for the detection system are also presented. This microfluidic system eliminates the need for expensive readout optics and opens the door to low-cost disposable devices.

## 1. Introduction

The same basic fabrication concepts and materials which have made microelectronics successful are now being adapted to obtain low-cost, small, high-performance biomedical devices, such as a microfluidic system for biomedical analysis, also referred to as a laboratory on a chip (lab-on-a-chip).<sup>(1)</sup> The implementation of lab-on-a-chip devices presents new and interesting technological challenges, and their capabilities in chemical analysis are outstanding. Microscopic versions of liquid-handling devices, including pumps, valves, volume measuring tools, chemical reactors, extractors, filters, mixers and even sophisticated chromatographic techniques, can all be implemented and integrated into the chips' design, thanks to microsystem technology which enables the fabrication of precise and small structures. Microsystems with integrated devices on this scale are

---

Corresponding author, e-mail address: gminas@dei.uminho.pt

usually referred as Micro Total Analysis Systems ( $\mu$ TAS). They allow a variety of analytical methods or process controls for simple mixtures with resolving powers similar to today's macro analytical systems.<sup>(2)</sup>

The microchip-based technology resembles that of microelectronic computer chips. The microchips can be produced using photolithography and chemical etching techniques that are similar to those used in the manufacture of integrated circuits.<sup>(3)</sup> Microchannels are etched into the chip substrate or produced by injection molding to carry fluids: chemical reagents and sample solutions. The substrate can be glass, quartz or silicon.

The small size and portability of lab-on-a-chip devices result not only in a reduction in the cost and time of analytical testing, but also in a significant improvement in laboratory safety. Spills, explosions and other laboratory accidents that can occur with conventional sample preparation techniques are no longer a problem. Since nanoliter quantities of organic solvents and samples are used, the costs associated with buying new reagents and disposing of used ones are negligible.<sup>(4)</sup> Moreover, since the lab-on-a-chip rather than a chemist performs the sample preparation, untrained personnel can accurately and precisely perform a complete analysis.

In this paper a microfluidic system designed for the determination of protein concentration (*e.g.*, albumin and total protein) in urine analysis is presented. The microsystem itself is composed of two wafers: one containing the microlaboratory and the other the protein concentration detection system. The detection system consists of color analysis based on optical absorption. The wavelength region over which the optical absorption is maximum or minimum for the different proteins is very narrow; consequently, a highly selective optical detector is needed.

## 2. Design of a System to Determine Protein Concentration

The process for determining protein concentration in a biological fluid is based on colorimetric detection. When proteins react with a specific reagent, an absorption maximum occurs at a specific wavelength for the mixture. This specific wavelength is dependent on the protein and the reagent.<sup>(5)</sup> As an example, for determining the total protein concentration in a sample of urine (usually called proteinuria) the reaction (sample plus reagent) has an absorption maximum at 600 nm, while for determining albumin (usually called albuminuria) the reaction has an absorption maximum at 628 nm.

Another method for determining protein concentration in a biological fluid and which is also practical for local laboratories is based on fluorometry rather than absorbance.<sup>(6,7)</sup> However, fluorometry has some disadvantages, such as: it is not easy to find a reagent that forms a strongly fluorescence complex; the absorption spectra has a wide bandwidth; the reaction has short lifetimes (< 500 ns), and a fluorescence excitation beam is necessary, while in the absorbance method, white light is sufficient. Therefore, the lab-on-a-chip described in this paper is designed for determining protein concentration by absorbance.

### 2.1 Protein absorption spectrum

To design and calibrate the detection system, some measurements need to be performed to determine the real transmitted wavelengths and the real relationship between protein

concentration and the intensity of the transmitted light. Measurements by colorimetric detection were performed in a 1 cm lightpath cuvette with a Model UV-3101PC SHIMADZU spectrophotometer. The experimental results were obtained by total protein and albumin analysis using reagents and protein standards from Sigma-Aldrich.<sup>(5)</sup> These reagents allow the detection of the protein concentration using absorbance.

Known protein concentrations were used to obtain calibration curves and several absorption spectra. Figure 1(a) shows the absorption spectra when different albumin concentrations react with microprotein-pr reagent (0.05 mmol/l pyrogallol red, 0.16 mmol/l sodium molybdate, buffer, chelating agent, stabilizer, surfactant and preservative<sup>(5)</sup>). The microprotein-pr reagent<sup>(8)</sup> is only suitable for quantifying the presence of total protein in urine (proteinuria), which can be a symptom of many renal disorders. Measurement results were obtained in the range from 10  $\mu\text{g/ml}$  to 500  $\mu\text{g/ml}$ , comprising the range of normal and usual abnormal values in a human being (the normal value is below 150  $\mu\text{g/dl}$ <sup>(9)</sup>). It can be seen that as the albumin concentration is reduced, the absorbance decreases. The results present linear behavior until 2 mg/ml.

If it is necessary to quantify very low levels of total protein (below 10  $\mu\text{g/ml}$ ), the Bradford reagent is used instead of the microprotein-pr reagent.<sup>(10,11)</sup> The mixture has an absorption maximum at 595 nm (Fig. 1(b)).

For quantifying only the presence of albumin, bromcresol green reagent (0.30 mmol/l, pH = 4.2) was used.<sup>(12)</sup> The mixture has an absorption maximum at 628 nm (Fig. 1(c)). However, with this reagent only albumin concentrations above 500  $\mu\text{g/ml}$  can be measured; it is generally used for serum or for very high levels in urine.

This kind of analysis suits the purpose of the lab-on-a-chip, and the device is thus very useful for an initial diagnostic in a patient's home.

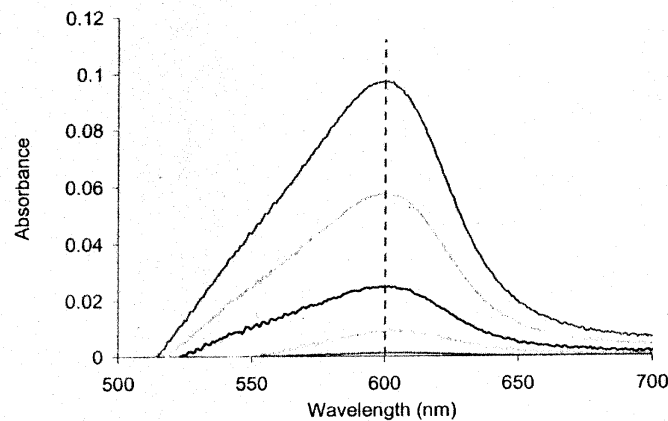


Fig. 1(a). Absorption spectra for different albumin concentrations after binding with microprotein-pr reagent. From top curve to bottom curve: 500  $\mu\text{g/ml}$ , 300  $\mu\text{g/ml}$ , 150  $\mu\text{g/ml}$ , 75  $\mu\text{g/ml}$ , 10  $\mu\text{g/ml}$ .

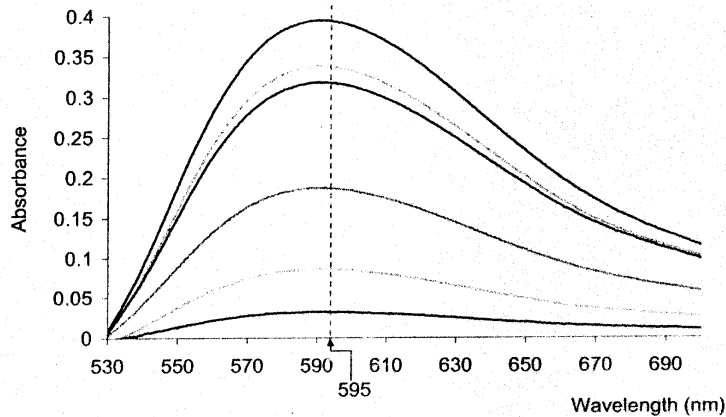


Fig.1(b). Absorption spectra for very low albumin concentrations (binding with Bradford reagent). From top curve to bottom curve: 9  $\mu\text{g/ml}$ , 7.5  $\mu\text{g/ml}$ , 7.1  $\mu\text{g/ml}$ , 4  $\mu\text{g/ml}$ , 2  $\mu\text{g/ml}$ , 1  $\mu\text{g/ml}$ .

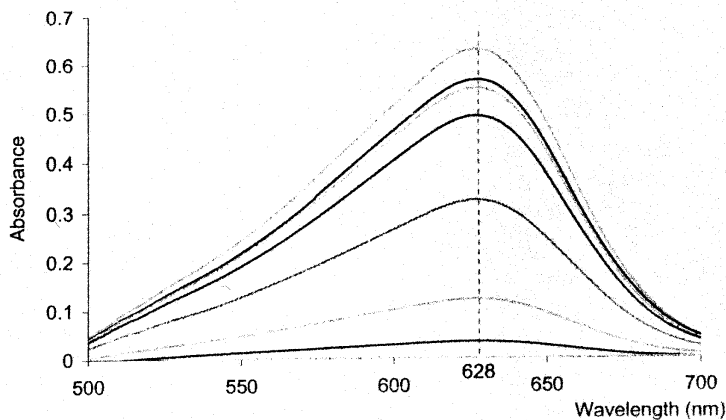


Fig.1(c). Absorption spectra for different albumin concentrations after binding with bromocresol green. From top curve to bottom curve: 50 mg/ml, 45 mg/ml, 44 mg/ml, 40 mg/ml, 25 mg/ml, 10 mg/ml, 5 mg/ml, 500  $\mu\text{g/ml}$ .

## 2.2 Discussion

From the previous spectra it can be concluded that the intensity of the color produced by the mixture is directly proportional to the protein concentration.

For the colorimetric detection, white light is used as incident light in the detection chamber, where some spectral components are absorbed. To select an effective wavelength (the specific wavelength at which the absorption is a maximum or a minimum) a Fabry-Perot filter is used.

### 2.3 Optical filter design

A Fabry-Perot filter consists of two parallel mirrors with a resonance cavity in the middle (Fig. 2).<sup>(13)</sup> The equation  $2nd = \lambda q$  shows its operation principle, where  $n$  is the refractive index of the cavity medium,  $d$  the cavity length,  $\lambda$  the incident wavelength and  $q$  the interference order ( $q = 1, 2, 3, \dots$ ). The optical transmission characteristic of such an element consists of a series of sharp resonant transmission peaks when the cavity length equals multiples of a half-wavelength of the incident light (with  $n = 1$ ). The intensity of the light transmitted through the Fabry-Perot filter is measured in the integrated photodiode and gives information about the protein concentrations.

The most important parts of the Fabry-Perot devices are the mirrors. Two types of highly reflective coatings are used in mirrors: dielectric and metallic. Dielectric mirrors, when properly designed and fabricated, have high performance characteristics (high reflectivity, low absorption losses). However, metallic mirrors can be attractive in certain applications due to the simplicity of their fabrication (only one layer is deposited). Another advantage is that metallic mirrors generally perform well over a wide spectral range. Aluminum, gold and silver are the most commonly used metals for reflective coatings. Figure 3 shows their reflectance in the visible spectral region.

Aluminum is the most suitable material in terms of fabrication compatibility, but unfortunately it has higher absorption losses than silver or gold in the visible region. For this spectral region, silver is the best choice, but it exhibits poor long-term stability (tendency to tarnish).<sup>(14)</sup> Gold is more corrosion resistant than silver but it has a poor performance in the visible region. Unlike macroscopic applications of silver-based reflective coatings, the poor environmental resistance of silver is not critical in a microsystem application, because the sealing of the complete system prevents any degradation of the mirror caused by the environment. Another advantage is that silver is a natural low-pass filter, cutting off the UV range (see Fig. 3). Therefore, and according to the simulation results (presented in section 4), the best option for a Fabry-Perot resonance cavity for the

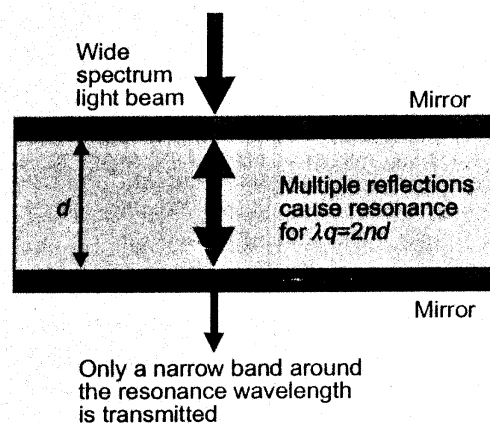


Fig. 2. Fabry-Perot filter.

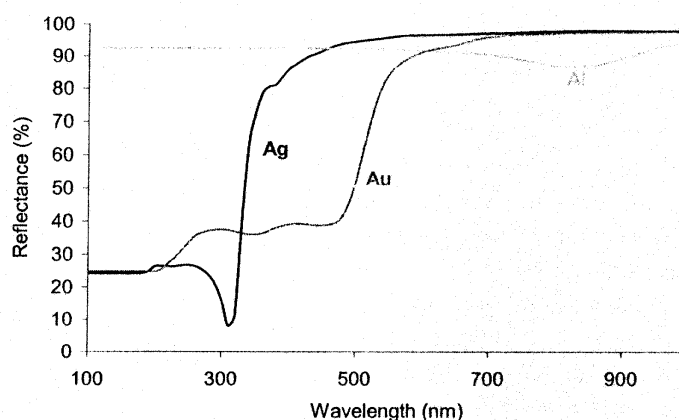


Fig. 3. Reflectance of aluminum, gold and silver as a function of the wavelength of the radiation.

visible range in terms of optical characteristics is to use two silver mirrors with a resonance cavity of PECVD  $\text{SiO}_2$  film (with a low and almost constant refractive index in the same range).

The main difference between the three mixtures analyzed occurs in the wavelength region in which they have an absorption maximum (see Figs. 1(a), 1(b) and 1(c)). From the operation principle of the Fabry-Perot filter, it can be seen that the wavelength selection is performed by changing the thickness of the cavity. Therefore, different labs-on-a-chip can be fabricated for different protein analyses based on the same principles and fabrication methods. The reaction time (which is different for each protein) can be controlled by the potential applied to the electrodes.

A lab-on-a-chip can perform different protein analyses, but this increases the complexity of the microfluidic system. An array of Fabry-Perot filters with the respective detectors underneath is required to cover a well-defined spectral range.

### 3. Optical Simulations of the Fabry-Perot Filter

A thin-film optics software package (TFCalc 3.3) was used for optimization of the Fabry-Perot filter, i.e., for selecting the materials and thickness of each layer. The simulations used the material data provided by the database of the Sopra Company.<sup>(15)</sup> For proteinuria detection (mixture measured in Fig. 1(a)) the transmittance of a 55 nm-Ag / 1185 nm- $\text{SiO}_2$  / 45 nm-Ag layer stack (Fig. 4(a)) shows a FWHM (full-width half-maximum) of 2.7 nm and a finesse (ratio between the free spectral range and FWHM) of 32. To achieve a single peak a commercial high-pass optical filter on top of the microsystem is used to cut a wide region of the spectrum (with a cut-off wavelength of 570 nm).

Figures 4(b) and 4(c) show the simulated transmittance of the Fabry-Perot filter for the quantification of very low levels of total protein (mixture measured in Fig. 1(b)) and for only albumin detection (mixture measured in Fig. 1(c)), respectively. The FWHM of

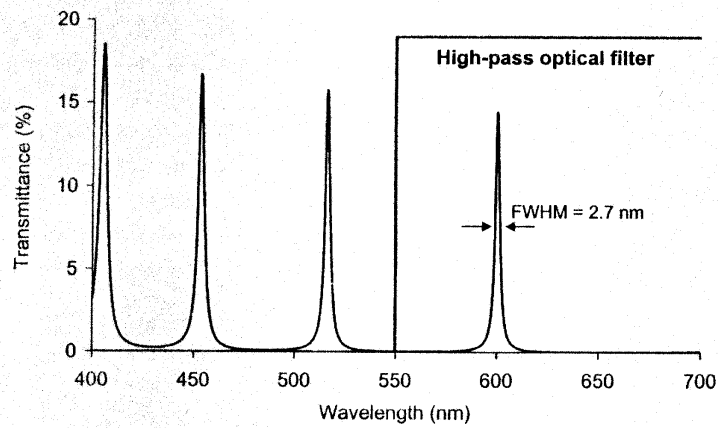


Fig. 4(a). Simulated transmittance vs. wavelength for a 55 nm-Ag / 1185 nm-SiO<sub>2</sub> / 45 nm-Ag layer stack.

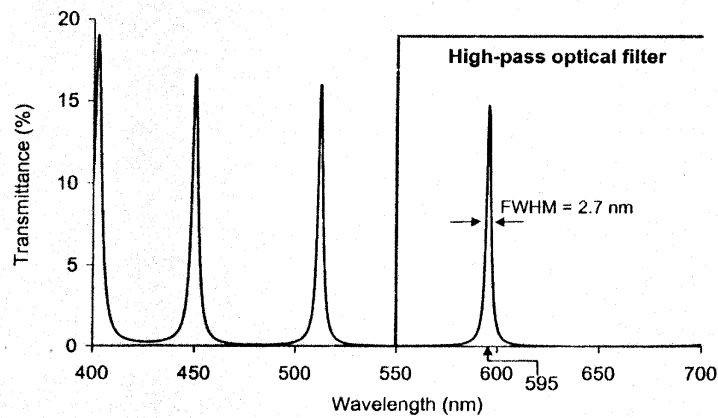


Fig. 4(b). Simulated transmittance vs. wavelength for a 55 nm-Ag / 1175 nm-SiO<sub>2</sub> / 45 nm-Ag layer stack.

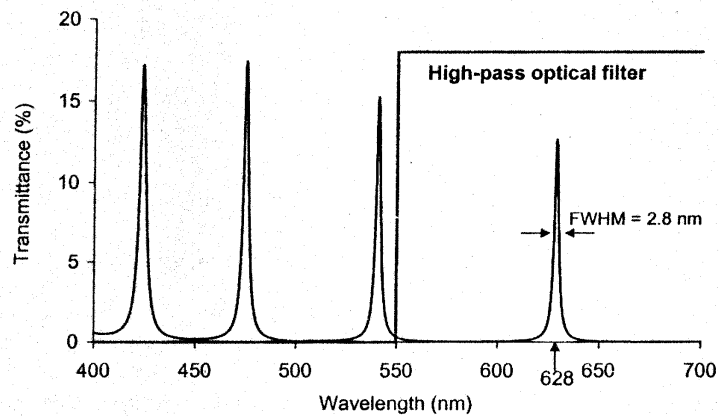


Fig. 4(c). Simulated transmittance vs. wavelength for a 55 nm-Ag / 1245 nm-SiO<sub>2</sub> / 45 nm-Ag layer stack.

2.7 nm and finesse of 30 were obtained as shown in Fig. 4(b), while in Fig. 4(c) these values were 2.8 nm and 36, respectively. Simulations show that it is possible to obtain the desired selectivity (Fig. 5) regarding the absorption spectrum measured in section 3.1.

The thickness of the silver layer is a trade-off between achievable FWHM and absorption losses. When aluminum is used for the bottom mirror (due to fabrication constraints), the performance decreases due to higher absorption of aluminum films compared to that of silver (Fig. 6). Values of FWHMs and finesesses of approximately 6.3 nm and 14 were achieved, respectively (using a 4<sup>th</sup> order Fabry-Perot filter). The

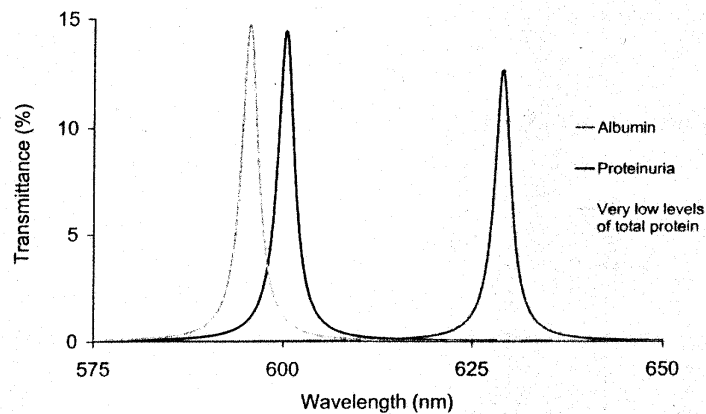


Fig. 5. Overlap of the simulated transmittances of Figs. 4(a), 4(b) and 4(c).

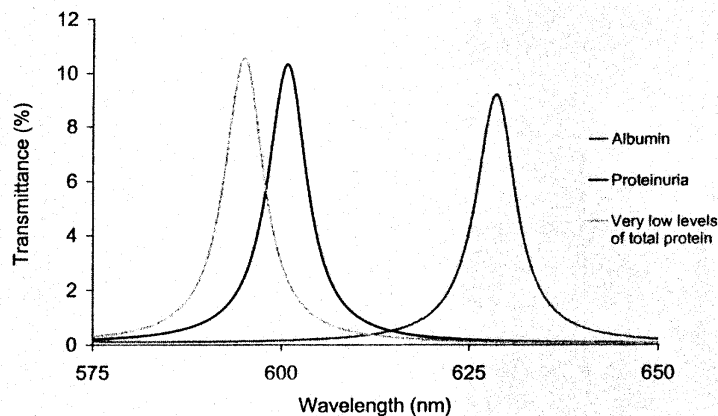


Fig. 6. Overlap of the simulated transmittance for the three mixtures with a 20 nm-Al / SiO<sub>2</sub> / 30 nm-Ag layer stack. The SiO<sub>2</sub> layer has 1180, 1195 or 1253 nm for very low levels of total protein, total protein and albumin detection, respectively.



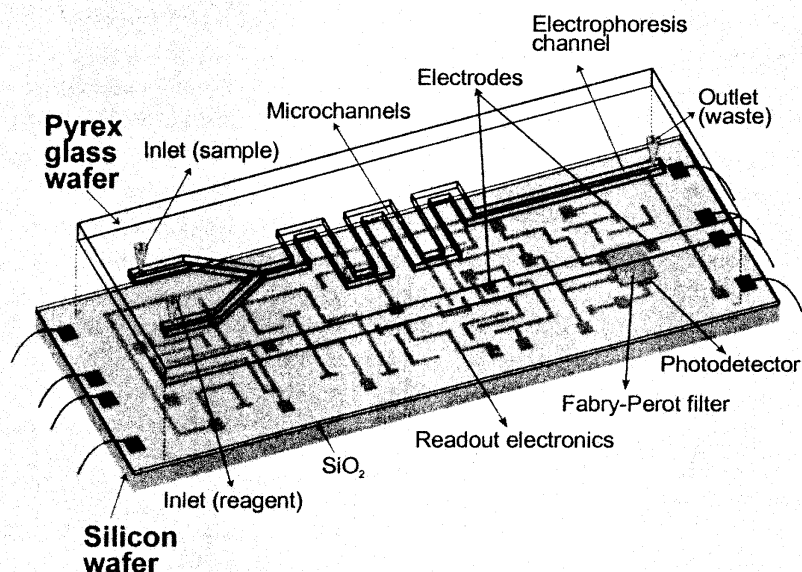


Fig. 7. Lab-on-a-chip: the top wafer contains the microchannels; the bottom wafer has the detection system and readout electronics.

FWHM could be decreased with a high-order filter. For example, with a 6<sup>th</sup> order Fabry-Perot filter FWHMs around 3.8 and finesses around 14 were obtained.

When the lab-on-a-chip is used, the lightpath is definitively smaller (around 500  $\mu\text{m}$ ), and the range of the transmittance between the reagent (solution without protein) and the higher protein concentration is also smaller. A theoretical study of the transmittance in a 500  $\mu\text{m}$  lightpath showed that, with a 12 bit analog-to-digital converter in the readout electronics, a sensitivity of 10  $\mu\text{g/ml}$  is achieved.

### 3.1 Compensation in the optical detection system

Any imperfection in the incident light wave in a real Fabry-Perot structure causes increased transmittance outside the narrow band to which the Fabry-Perot filter is tuned (parasitic background signal). The addition of a compensation structure with the optical length of the cavity below  $\lambda/10$  is a possible solution. The transmittance is similar to the parasitic background and is subtracted from the real signal.

## 4. Lab-on-a-Chip Design

Figure 7 shows the design of the lab-on-a-chip. The microlaboratory (top wafer) consists of a Pyrex glass top wafer with wet-etched microchannels for carrying chemical reagents and sample solutions. Glass was chosen for its transparency and because it is an electrical insulator.<sup>(16)</sup> Therefore, electrophoretic flow principles can be used to move fluids through the microchannels; this avoids the need for mechanical pumps and valves.

Thus, fluid movement results from electrokinetic forces derived from small voltages that are applied to specific regions in the microsystem.

The device consists of two microchannels (from inlets 1 and 2) merging into one (to outlet 3). Sample and reagent solutions are injected in the lab-on-a-chip through inlets and both solutions are mixed in the main microchannel. Low voltages are applied between electrodes (on the silicon wafer) distributed by the flow path.

The mixture is analyzed by a pn-junction photodetector fabricated in silicon under the microchannel. The Fabry-Perot filter is placed above the photodetector. It was designed to show clearly the maximum absorbance in the wavelength specific for each reagent (see section 3 and Figs. 4 to 6). The photodetector and respective readout electronics are fabricated by a CMOS standard process. The layers of the Fabry-Perot filter are deposited at the very end of the fabrication sequence. The silver layer is patterned using lift-off. Both wafers are bonded by a glass-to-silicon anodic bonding process which is already widely utilized in the fabrication of microchemical devices.<sup>(17-19)</sup> The process has a low bonding temperature and no aggressive chemicals are used.

Some protein detection requires a capillary electrophoresis separation technique (*e.g.*, amino acid detection). This lab-on-a-chip can also perform such techniques by application of a high voltage across the main microchannel.

## 5. Experiments Using a 1 mm Lightpath Cuvette

Figure 8 shows the experimental arrangement used for determining total protein concentration when a 1 mm lightpath glass cuvette is placed above a pn-junction photodetector (while the integrated microfluidic system is being fabricated). The optical response was measured with a HP4142B DC source/monitor (full scale range from  $10^{-15}$  A to 1 A and a

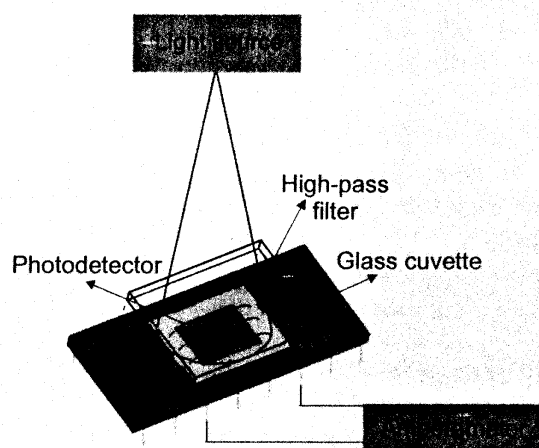


Fig. 8. Experimental arrangement used in the 1 mm lightpath cuvette measurements (100  $\mu$ l of liquid volume).

resolution of  $10^{-13}$  A). A 100 W quartz tungsten halogen lamp with a monochromator TRIAX-180 (1200 g/mm grating with a spectral dispersion of 3.6 nm/mm and a spectral resolution of 0.3 nm at 546 nm) was used as light source. Measurements (presented in Fig. 9) were performed for the same reagent and protein concentration as devised for Fig. 1.

When the simulated Fabry-Perot filter shown in Fig. 6 is placed between the cuvette and of the photodetector, its current response will be similar to the one illustrated in Fig. 10. It can be seen that due to the presence of the Fabry-Perot filter (Fig. 6), the magnitude of the electric current measured by the photodetector decreases by a factor of

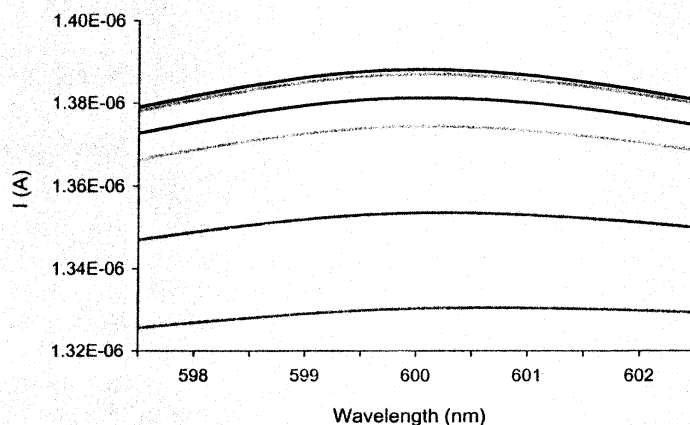


Fig. 9. Current measured by the photodetector (without filter) for the same solutions as Fig. 1 using a 1 mm lightpath cuvette. From top curve to bottom curve: reagent,  $10 \mu\text{g/ml}$ ,  $75 \mu\text{g/ml}$ ,  $150 \mu\text{g/ml}$ ,  $300 \mu\text{g/ml}$ ,  $500 \mu\text{g/ml}$ .

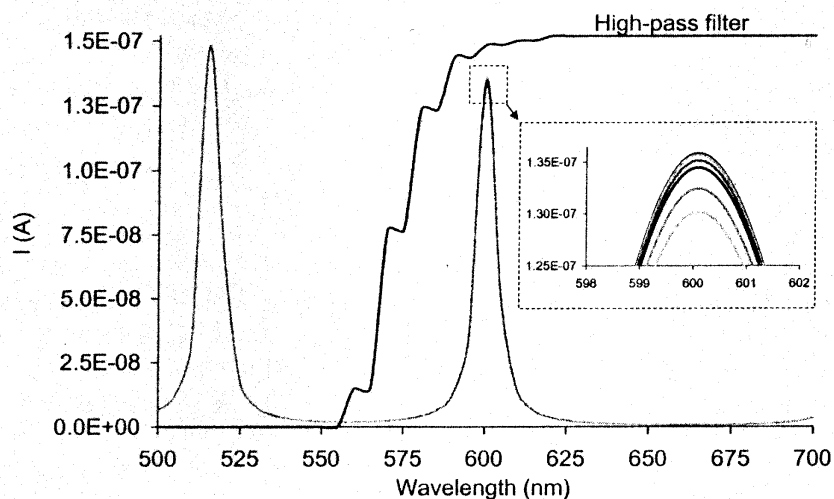


Fig. 10. Simulated photodiode current when the Fabry-Perot filter in Fig. 6 is used between the photodiode and the cuvette. From top curve to bottom curve: reagent,  $10 \mu\text{g/ml}$ ,  $75 \mu\text{g/ml}$ ,  $150 \mu\text{g/ml}$ ,  $300 \mu\text{g/ml}$ ,  $500 \mu\text{g/ml}$ .

10. A commercial high-pass filter (OG570 from Schott) is used on top of the microsystem to achieve a single peak. As the albumin concentration is increased, the photodiode current is decreased (in the neighborhood of 600 nm). The difference in the photodiode current between the adjacent concentrations is very small (around 100 pA), which leads to very accurate readout electronics. However, if the lamp power is increased, the performance of the readout electronics will become easier.

Moreover, tests using a lightpath smaller than 1 mm are being carried out in order to reduce the liquid volume.

## 6. Conclusions

The lab-on-a-chip described in this paper presents a high level of automation, real-time analysis and the possibility of *in situ* measurements (at a patient's home, for example). It also has the advantage of having an accurate volume inlet which eliminates the problem of manual pipetting; that is, if two different people pipet solutions of the same concentration the results may not be the same.

The optical detection system is highly sensitive to specific wavelengths according the Fabry-Perot filter design. A FWHM of 2.7 nm and finesse of 32 were achieved in proteinuria determinations (if it is not necessary that aluminum be used for the bottom mirror), otherwise these values were 6.3 nm for FWHM and 14 for finesse. Moreover, tests using ambient light have been carried out to avoid the use of a known source of light. Therefore, this detection system is extremely suitable for application in microfluidics systems (*e.g.*,  $\mu$ TAS) due to its small size and highly selective optical detection.

Although this microsystem was presented for urine analysis, other biological fluids (such as serum, sweat, saliva or cerebrospinal fluid) are potential candidates for the lab-on-a-chip.

Other applications of the lab-on-a-chip are for monitoring the air and the water quality for potential toxins and pesticides, screening foods, and promptly identifying drugs of abuse. Lab-on-a-chip devices will probably be applied in forensic, environmental and food testing laboratories in the near future. Moreover, since low quantities of hazardous chemical reagents are needed, the resultant environmental pollution is no longer a problem.

## Acknowledgements

The authors wish to acknowledge the cooperation with Professor R. F. Wolffenbuttel's group from the Laboratory for Electronic Instrumentation, TUDelft, The Netherlands. We also thank C. Pereira from the Biology Dept., University of Minho, Portugal for her help with the test kits, as well as M. Rui from the Physics Dept. of the same University for the use of the spectrophotometer. This work is supported by the Foundation of Science and Technology, Portugal, FCT, POCTI/33747/ESE/2000 and FEDER.

## References

- 1 M. D. Mangriotis, S. S. Mehendale, T. Z. Liu, A. M. Jacobi, M. A. Shannon and D. J. Beebe: Proc. of TRANSDUCERS'99 (Sendai, Japan, 1999).
- 2 C. H. Mastrangelo, M. A. Burns and D. T. Burke: Proc. of the IEEE, 86-8 (1998) 1769.
- 3 A. Manz and H. Beckert: *Microsystem Technology in Chemistry and Life Sciences* (Springer, New York, 1999) p. 1.
- 4 P. C. Simpson, A. T. Woolley and R. A. Mathies: *Biomedical Microdevices* **1** (1998) 7.
- 5 *Biochemistry and Organic Reagents: for bioscience investigation* (Sigma, 2000).
- 6 M. A. Kessler and O. S. Wolfbeis: *Analytical Biochemistry* **200** (1992) 254.
- 7 M. A. Kessler, A. Meinitzer, W. Petek and O. S. Wolfbeis: *Clinical Chemistry* **43** (1997) 996.
- 8 N. Watanabe, et al.: *Clinical Chemistry* **32** (1986) 1551.
- 9 F. T. Fischbach: *A Manual of Laboratory & Diagnostic Tests* (Lippincott Raven Publishers, USA, 1996).
- 10 M. M. Bradford: *Analytical Biochemistry* **72** (1976) 248.
- 11 J. J. Sedmak and S. E. Grossberg: *Analytical Biochemistry* **79** (1977) 544.
- 12 J. Savory, M. G. Heintges, M. Sonowane and R. E. Cross: *Clinical Chemistry* **22** (1976) 1102.
- 13 B. Saleh and M. C. Teich: *Fundamentals of Photonics* (J. Wiley & Sons, 1991).
- 14 D. Y. Song, R. W. Sprague, H. A. MacLeod and M. R. Jacobson: *Applied Optics* **24** (1985) 1164.
- 15 Optical properties of coating materials from SOPRA S.A., Web site: <http://www.sopra-sa.com/indices.htm>, 2000.
- 16 J. C. Rouler, K. Fluri, E. Verpoorte, R. Völkel, H. P. Herzig, N. F. Rooij and R. Dändliker: Proc. of TRANSDUCERS'99 (Sendai, Japan, 1999).
- 17 B. H. Schoot, H. H. Vlekkert, N. F. Rooij, A. Berg, and A. Grisel: *Sensors and Actuators B4* (1991) 239.
- 18 U. Lehmann, O. Krusemark and J. Mueller: Proc. of  $\mu$ TAS 2000 (Enschede, The Netherlands, 2000) p. 167.
- 19 S. Matsumoto, A. Klein and R. Maeda: Proc. of  $\mu$ TAS 2000 (Enschede, The Netherlands, 2000) p. 183.